

Article

Binding of Arsenic by Common Functional Groups: An Experimental and Quantum-Mechanical Study

Donatella Chillé ^{1,†}, Viviana Mollica-Nardo ^{2,†}, Ottavia Giuffré ¹, Rosina Celeste Ponterio ², Franz Saija ², Jiří Sponer ³, Sebastiano Trusso ², Giuseppe Cassone ^{2,*} and Claudia Foti ^{1,*}

¹ Dipartimento di Scienze Chimiche, Biologiche, Farmaceutiche ed Ambientali, Università degli Studi di Messina, Salita Sperone 31, 98166 Messina, Italy; donatella.chille@unime.it (D.C.); ogiuffre@unime.it (O.G.)

² Institute for Chemical-Physical Processes, National Research Council of Italy (IPCF-CNR), V.le F. Stagno d'Alcontres 37, 98158 Messina, Italy; mollica@ipcf.cnr.it (V.M.-N.); ponterio@ipcf.cnr.it (R.C.P.); saija@ipcf.cnr.it (F.S.); trusso@ipcf.cnr.it (S.T.)

³ Institute of Biophysics, Czech Academy of Sciences (IBP-CAS), Královopolská 135, 61265 Brno, Czech Republic; sponer@ncbr.muni.cz

* Correspondence: cassone@ipcf.cnr.it (G.C.); cfoti@unime.it (C.F.)

† These authors contributed equally to this work.

Citation: Chillé, D.; Mollica-Nardo, V.; Giuffré, O.; Ponterio, R.C.; Saija, F.; Sponer, J.; Trusso, S.; Cassone, G.; Foti, C. Binding of Arsenic by Common Functional Groups: An Experimental and Quantum-Mechanical Study. *Appl. Sci.* **2022**, *12*, 3210. <https://doi.org/10.3390/app12063210>

Academic Editor: Raed Abu-Reziq

Received: 15 February 2022

Accepted: 18 March 2022

Published: 21 March 2022

Publisher's Note: MDPI stays neutral with regard to jurisdictional claims in published maps and institutional affiliations.



Copyright: © 2022 by the authors. Licensee MDPI, Basel, Switzerland. This article is an open access article distributed under the terms and conditions of the Creative Commons Attribution (CC BY) license (<http://creativecommons.org/licenses/by/4.0/>).

Abstract: Arsenic is a well-known contaminant present in different environmental compartments and in human organs and tissues. Inorganic As(III) represents one of the most dangerous arsenic forms. Its toxicity is attributed to its great affinity with the thiol groups of proteins. Considering the simultaneous presence in all environmental compartments of other common functional groups, we here present a study aimed at evaluating their contribution to the As(III) complexation. As(III) interactions with four (from di- to hexa-) carboxylic acids, five (from mono- to penta-) amines, and four amino acids were evaluated via experimental methods and, in simplified systems, also by quantum-mechanical calculations. Data were analyzed also with respect to those previously reported for mixed thiol-carboxylic ligands to evaluate the contribution of each functional group (-SH, -COOH, and -NH₂) toward the As(III) complexation. Formation constants of As(III) complex species were experimentally determined, and data were analyzed for each class of ligand. An empirical relationship was reported, taking into account the contribution of each functional group to the complexation process and allowing for a rough estimate of the stability of species in systems where As(III) and thiol, carboxylic, or amino groups are involved. Quantum-mechanical calculations allowed for the evaluation and the characterization of the main chelation reactions of As(III). The potential competitive effects of the investigated groups were evaluated using cysteine, a prototypical species possessing all the functional groups under investigation. Results confirm the higher binding capabilities of the thiol group under different circumstances, but also indicate the concrete possibility of the simultaneous binding of As(III) by the thiol and the carboxylic groups.

Keywords: arsenic interactions; -S, -N, and -O donor ligands; complex formation constants; quantum-mechanical calculations; binding mechanisms

1. Introduction

Arsenic (As) is an element easily detectable in the environment as a consequence of many natural and anthropogenic activities. It is a minor but ubiquitous element of the Earth's crust, and some chemical species are volatile and highly soluble in aquatic systems. In general, arsenite and arsenate minerals are highly soluble in aqueous solution, often proving to be sources of arsenic contamination [1–5].

The effects of arsenic compounds on humankind are strictly related to contamination. In fact, from the environment arsenic may reach the human organism through many

pathways: by inhalation, responsible for respiratory system problems; by dermal exposure, which can lead to lesions and aggressive skin cancers; or by ingestion of contaminated foods and water. In particular, the latter, i.e., the consumption of As-contaminated drinking water, is considered—among the As-induced diseases—as the primary cause of human illness, and in 1992, this prompted the World Health Organization (WHO) to reduce the recommended value for arsenic in drinking water from 50 µg/L (fixed value in 1963) to 10 µg/L, as a consequence of the suspicion of carcinogenicity. Arsenic is nowadays recognized as one of the most dangerous pollutants, and the International Agency of Research on Cancer (IARC) classified it as a class I carcinogen that exhibits acute and chronic toxicity depending on the type of exposure [6]. Ingestion of large doses of arsenic leads to cardiovascular, gastrointestinal, and central nervous system disorders and, in some cases, to death. Chronic arsenic exposure represents a serious public health concern because As affects almost all organ systems, resulting in diseases of the vascular, respiratory, neurological, reproductive, and endocrine systems and causing tumors of the skin, lung, and urinary bladder [6,7], in addition to an increased risk of diabetes mellitus. Despite the carcinogenic potential of arsenic has been widely studied, the mechanisms by which it causes cancer and other diseases remain poorly understood.

Similarly to other chemical elements, toxicity strongly depends on the arsenic speciation, i.e., on the form under which it is present in different environmental compartments and human organs and tissues. As shares properties with both metals and nonmetals, and it is thus classified as a metalloid. It holds four oxidation states (-3, 0, +3, +5) and can be found in a variety of inorganic and organic forms exhibiting different toxicities and bioavailability [8]. Distinguishing between species is important due to the differences in properties and mechanisms of toxicity. Different species have different toxicity and bioavailability, but the knowledge of the speciation is also important to define and develop suitable removal procedures [1,9–13]. Inorganic As(III) represents the most toxic arsenic form because of its high affinity toward sulfhydryl groups of proteins. Recently, in order to evaluate the strength of As(III)–SH interactions, experimental and computational investigations have been performed on mixed thiol-carboxylic ligands (thiol, thiomalic, and dimer-captosuccinic acids) [14,15]. Notwithstanding these studies confirmed the pronounced As(III)–thiol group interaction, they also evidenced the contribution of carboxylate groups to the whole stabilization of complex species.

In light of this, the study on the interactions established by As(III) with some important functional groups typically present in proteins (carboxylic and amino) has been undertaken to evaluate their contribution to the stability of the formed complexes. Three classes of ligands were taken into account: simple carboxylic acids and linear amines, but also amino acids to evaluate the presence of carboxylic and amino groups simultaneously. Carboxylic acids are compounds naturally involved in different stages of life cycles, but they can also be synthesized industrially by oxidation reaction of aldehyde or primary alcohol as well. Their application fields are disparate and include medicine, food, pharmaceutical and other industries (production of polymers, coatings, and adhesives) [16]. In the food industry, they can be used as additives to lend specific organoleptic properties or stability to the food, although some type of acids, such as citric acid, tartaric acid, or malic acid, occur naturally in foods such as fruit [17]. Amines are nitrogen-bearing compounds obtained by microbial decarboxylation of amino acids. Since these microorganisms are commonly present in the environment, amines can be contained in food and beverages. Their concentration is higher in easily perishable foods, especially fermented food or foods rich in amino acids, such as fish, meat, wine, dairy, and cheese. Amino acids represent the constitutive units of the proteins, and, for this, they are defined as proteino-genic. Some of them, not synthesized by the human organism, must be taken through food; these ones are indicated as “essential amino acids” [18].

The aim of this paper is that of evaluating the strength of each As(III)–ligand interaction and of determining the contribution of each functional group to the stabilization process in a competitive environment where all donor groups are present. The ligands under

study, reported in Figure 1, were chosen with the aim of having different number of functional groups within the same class of ligands (from di- to hexa-carboxylic acids and from mono- to penta-amines) and different combinations of functional groups: glycine with one carboxylic and one amino group, aspartic with two carboxylic, lysine with two amino groups, together with cysteine, in which a sulfhydryl group is also present. Data were evaluated together with those previously reported on mixed thiol-carboxylic ligands (*tla*, *tma*, and *dmsa*) [14,15].

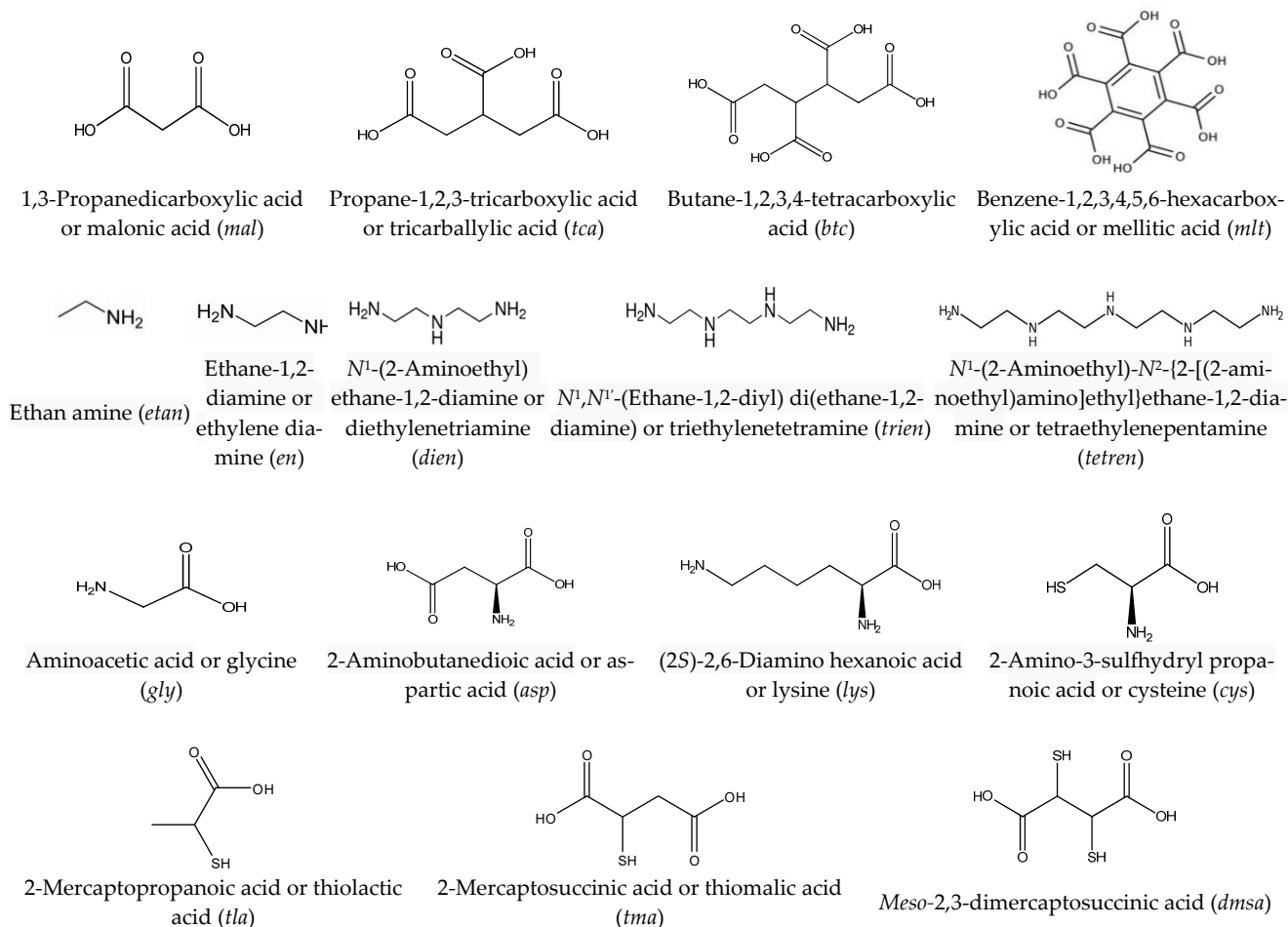


Figure 1. Ligands under study.

2. Materials and Methods

2.1. Reagents

Sodium (meta)arsenite salt (Sigma-Aldrich, $\geq 90\%$) was weighed and solubilized for the preparation of As(III) solutions. Aminoacids solutions were prepared, without further purification, by weighing glycine (*gly*), purchased from Sigma-Aldrich; L-aspartic acid (*asp*); and L-lysine (*lys*) in the chloridrate form, both purchased from Fluka. As regards carboxylic acids, 1,3-propanedicarboxylic acid or malonic acid (*mal*), propane-1,2,3-tricarboxylic acid or tricarballic acid (*tca*), butane-1,2,3,4-tetracarboxylic acid (*btc*) and benzenhexacarboxylic acid or mellitic acid (*mlt*), bought from Fluka, were used for the preparation of the corresponding solutions by following the same methodology previously reported. Amine solutions were prepared by weighing the products. Ethylenediamine (*en*) and diethylenetriamine (*dien*) were bought from Fluka (purity $>97\%$). Ethanamine dihydrochloride, triethylenetetramine (*trien*) tetrachlorhydrate, and tetraethylenepentamine (*tetren*) pentachlorhydrate are Aldrich products (purity 98%).

Standard solutions of HCl and NaOH were obtained from concentrated Fluka ampoules and titrated with sodium carbonate and potassium biphthalate, respectively. Both salts were previously dried in an oven at 383 K for at least an hour. Moreover, to preserve sodium hydroxide solutions from CO₂, dark bottles equipped with a soda lime trap were used for the storage. Sodium chloride Fluka salt was weighed for the preparation of the corresponding solutions after drying in an oven at 383 K. For the preparation of all the solutions, grade A glassware and bi-distilled water were employed.

2.2. Potentiometric Equipment and Procedure

A Metrohm model 809 Titrando potentiometer provided with an Orion-Ross 8102 combined glass electrode and an automatic dispenser Metrohm Dosino 800 was employed to carry out potentiometric measurements. The potentiometric system has an estimated error of ± 0.15 mV for e.m.f. and ± 0.002 mL for titrant volume readings, and it is connected with a PC provided by TIAMO 2.2 software able to manage titrant delivery, e.m.f. stability, and data acquisition.

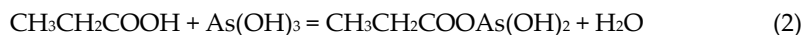
As for the carboxylate systems, 25 mL of the solution containing As(III) ($1 \leq C_{As} \leq 8$ mmol/L) and the ligand under study [*mal* ($1.5 \leq C_{mal} \leq 10$ mmol/L) or *tca* ($2 \leq C_{tca} \leq 10$ mmol/L) or *btc* ($2 \leq C_{btc} \leq 10$ mmol/L) or *mlt* ($2 \leq C_L \leq 8$ mmol/L)], acidified with HCl ($3 \leq C_{HCl} \leq 10$ mmol/L), was titrated with standard NaOH. As for the amine systems, 25 mL of the solution containing As(III) ($1 \leq C_{As} \leq 3$ mmol/L), acidified only for *en* and *dien* systems with HCl ($3 \leq C_{HCl} \leq 12$ mmol/L), was titrated in presence of *etan* ($1 \leq C_{etan} \leq 6$ mmol/L) or *en* ($1 \leq C_{en} \leq 6$ mmol/L) or *dien* ($1 \leq C_{dien} \leq 3$ mmol/L) or *trien* ($1 \leq C_{trien} \leq 3$ mmol/L) or *tetren* ($1 \leq C_{tetren} \leq 3$ mmol/L). As for the amino acids systems, titrations were performed on 25 mL of the solution containing As(III) ($3 \leq C_{As} \leq 6$ mmol/L), *gly* or *lys* or *asp* ($2 \leq C_L \leq 10$ mmol/L), and HCl ($3 \leq C_{HCl} \leq 10$ mmol/L). In all systems, experimental measurements were performed in the pH 2–10 range, in NaCl as ionic medium at $I = 0.15$ mol/L.

Thermostatted glass jacket cells ensured a constant temperature of 298 K during the experiments, and the solutions were magnetically stirred and kept under nitrogen atmosphere in order to avoid the presence of O₂ and CO₂ inside. For determining the standard electrode potential, E^0 , and pK_w values in the same experimental conditions of ionic strength and temperature, HCl was titrated with standard NaOH. Potentiometric titrations were elaborated by employing the BSTAC and STACO computer programs [19], which for the obtaining of the formal potential E^0 , the liquid junction potential coefficient j_a , $E_j = j_a [H^+]$, and the stability constants. Moreover, they are able to check the concentration of the used reagents.

2.3. Quantum-Mechanical Calculations

Static quantum-mechanical calculations were performed by means of the Gaussian 09 software [20]. This software enables the evaluation of the ground-state structures along with the associated potential energy of selected molecular species. In this work, optimization of all the investigated molecular structures was performed by means of the hybrid B3LYP [21–24] Density Functional Theory (DFT) exchange and correlation functional. Geometry optimizations of the molecular structures were executed under implicit solvation employing the 6-311++G(d,p) atomic basis set for all atoms. As far as the simulation of the solvent is concerned, the conductive polarizable continuum model (CPCM) [25] was employed by setting parameters mimicking the water electrostatics. This way, geometrical relaxations at the ground-state of several structures were executed with the aim of quantifying the energetic gain associated with a series of chelation reactions between the investigated functional groups (i.e., thiol, amino, and carboxylic) and typical arsenic-bearing species present in aqueous solutions such as arsenous acid (As(OH)₃). In particular, the following de-hydration reactions have been considered and energetically characterized:





For the sake of completeness, a series of reactions involving the binding of the amino group toward arsenous acid was also executed. However, because the related reactions contain charged species, the comparison of its energetics with those of reactions (1) and (2) is certainly disputable. In fact, the ΔE value emerging from this analysis in the presence of charged entities is biased by the fact that screening effects are only poorly handled by continuum models of water and by the evidence that comparing energy differences between “neutral” reactions, such as reactions (1) and (2), with those emerging from “charged” processes renders the absolute energetic ground-state (reference) as ill-defined, from which energies are determined and, hence, makes questionable any stability ranking coming out from this specific analysis. With the aim of exploring a series of alternative “neutral” reactions involving the complexation of As(III) by the amino group, reactions such as $\text{CH}_3\text{CH}_2\text{NH}_2 + \text{As}(\text{OH})_3 = \text{CH}_3\text{CH}_2\text{NH}_2\text{As}(\text{OH})_3$ and $\text{CH}_3\text{CH}_2\text{NH}_2 + \text{As}(\text{OH})_3 = \text{CH}_3\text{CH}_2\text{NH}_3\text{OAs}(\text{OH})_2$ were also investigated. However, products of these reactions appear to be completely unstable since neither local nor global energy minima have been found.

Finally, with the aim of evaluating the chelation capabilities of the SH, NH₂, and COOH functional groups toward As(III), structural optimization—conducted at the B3LYP/6-311++G(d,p) level under implicit water solvation (CPCM)—of cysteine bound to arsenic-bearing species was performed as well. Cysteine was chosen as a prototypical molecule containing all the three functional groups here investigated so as to evaluate eventual competitive effects between them in the complexation process of As(III). In particular, all possible permutations of binding were considered, from the direct one-to-one (1,1) interaction between each functional group and As-bearing species up to the simultaneous threefold coordination (3,1) of As(III) with the thiol, amino, and carboxylic groups, passing through the two-to-one (2,1) interaction involving two groups at a time binding As(III). This way, quantum-mechanical calculations of seven systems constituted of cysteine+As(III)-bearing complexes were conducted in addition to the above-mentioned reactions. Consideration of dimers or trimers of cysteine binding As(III) will be considered as a future work since it would also require the employment of prolonged and computationally very demanding *ab initio* molecular dynamics simulations, similarly to those reported for simple thioacids in water by some of ours (see [14]).

3. Results

3.1. As(III)–Ligand Interactions

The interactions between As(III) and each ligand were determined by potentiometric titrations. Data were elaborated taking into account the acid–base behavior of As(III) [26] and of the ligands at the same ionic strength and temperature conditions (in NaCl at $I = 0.15$ mol/L and $T = 298.15$ K). As is known from the literature [26], As(III) in water is present as $\text{As}(\text{OH})_3$ but, for the sake of simplicity, it will be denoted as As throughout the manuscript. Literature data are summarized in Table S1 of the Supplementary Materials. Considering the extremely variable concentration of As(III) in natural systems, experimental measurements were performed, varying the concentration of arsenic; the concentration of ligands; and, above all, their concentration ratio, in order to evaluate the possible formation of species with different stoichiometries. In any case, for each class of ligands, the speciation models were featured by simple As–ligand species with different protonation degrees (AsLH_i species, with $0 \leq i \leq 5$). Results are resumed in Table 1, where the formation constant values $\log\beta$ referred to the overall formation equilibria are reported.

To evaluate the stability of the species, in Table 2, data are reported as stepwise formation constants $\log K$ ($\text{As}(\text{OH})_3 + \text{H}_i\text{L}$). As can be observed, in the presence of carboxylic or amino groups, the stability of the species is always weak, with $\log K$ values falling in the range $0.83 \leq \log K \leq 3.85$. To better analyze the data, Table 2 also reports the total number of carboxylic (n_{COOH}), amino (n_{NH_2}), and thiol (n_{SH}) groups in the molecule. In light of

this, some general considerations can be made on the different ligand groups. Among the carboxylates, stability of the species generally increases with the n_{COOH} values and, therefore, from the di- (*mal*) to the hexa-carboxylic acids (*mlt*). Quantum-mechanical calculations simulated on a prototypical monocarboxylic species, and reported later in the text, show the displacement of the OH group in $\text{As}(\text{OH})_3$ by the carboxylate, which directly binds to As(III).

For *mlt*, the increase of the stability with the number of deprotonated carboxylic groups (hence from the AsLH_2 to AsL species) can probably be attributed to the involvement of many groups to the coordination (chelate effect). To highlight this, in Table 2, the number of deprotonated COO^- groups (n_{COO^-}) is also reported.

Table 1. Overall stability constants for As(III)–ligand systems in NaCl at $I = 0.15$ mol/L and $T = 298.15$ K.

L	Species ^{a)}	log β	L	Species ^{a)}	log β	L	Species ^{a)}	log β
<i>mal</i>	AsL	1.44 ± 0.01 ^{b)}	<i>etan</i>	AsLH	12.22 ± 0.05 ^{b)}	<i>gly</i>	AsLH	10.40 ± 0.08 ^{b)}
	AsLH	6.27 ± 0.02						
<i>tca</i>	AsL	1.39 ± 0.04	<i>en</i>	AsLH	12.12 ± 0.03	<i>asp</i>	AsLH	10.79 ± 0.02
	AsLH	7.22 ± 0.02		AsLH ₂	19.76 ± 0.03		AsLH ₂	15.39 ± 0.03
	AsLH ₂	11.78 ± 0.02	<i>dien</i>	AsLH ₂	20.84 ± 0.04	<i>lys</i>	AsLH	13.00 ± 0.02
<i>btc</i>	AsLH	7.54 ± 0.02		AsLH ₃	25.91 ± 0.03		AsLH ₂	21.85 ± 0.04
	AsLH ₂	12.76 ± 0.02	<i>trien</i>	AsLH ₂	21.47 ± 0.03	<i>cys</i>	AsL	4.45 ± 0.04
	AsLH ₃	17.05 ± 0.01		AsLH ₃	28.96 ± 0.03		AsLH	13.47 ± 0.03
<i>mlt</i>	AsL	3.23 ± 0.02		AsLH ₄	33.28 ± 0.04		AsLH ₂	21.89 ± 0.04
	AsLH	8.69 ± 0.01	<i>tetren</i>	AsLH ₄	34.43 ± 0.02			
	AsLH ₂	13.34 ± 0.03		AsLH ₅	37.97 ± 0.02			

^{a)} As=As(III), ^{b)} \pm standard deviation.

Table 2. Stepwise formation constants of As(III)–ligand species in NaCl at $I = 0.15$ mol/L and $T = 298.15$ K.

L	Species ^{a)}	n_{SH}	n_{COOH}	n_{NH_2}	$n_{\text{S-}}$	$n_{\text{COO-}}$	n_{NH_3+}	logK ^{b)}
<i>mal</i>	AsL	0	2	0	0	2	0	1.44
	AsLH	0	2	0	0	1	0	1.05
<i>tca</i>	AsL	0	3	0	0	3	0	1.39
	AsLH	0	3	0	0	2	0	1.40
	AsLH ₂	0	3	0	0	1	0	1.45
<i>btc</i>	AsLH	0	4	0	0	3	0	1.33
	AsLH ₂	0	4	0	0	2	0	1.45
	AsLH ₃	0	4	0	0	1	0	1.66
<i>mlt</i>	AsL	0	6	0	0	6	0	3.23
	AsLH	0	6	0	0	5	0	2.30
	AsLH ₂	0	6	0	0	4	0	1.72
<i>etan</i>	AsLH	0	0	1	0	0	1	1.56
<i>en</i>	AsLH	0	0	2	0	0	1	2.18
	AsLH ₂	0	0	2	0	0	2	2.72
<i>dien</i>	AsLH ₂	0	0	3	0	0	2	2.00
	AsLH ₃	0	0	3	0	0	3	2.87

<i>trien</i>	AsLH ₂	0	0	4	0	0	2	2.68
	AsLH ₃	0	0	4	0	0	3	3.58
	AsLH ₄	0	0	4	0	0	4	3.85
<i>tetren</i>	AsLH ₄	0	0	5	0	0	4	2.67
	AsLH ₅	0	0	5	0	0	5	3.52
<i>gly</i>	AsLH	0	1	1	0	1	1	0.83
<i>asp</i>	AsLH	0	2	1	0	2	1	1.16
	AsLH ₂	0	2	1	0	1	1	2.32
<i>lys</i>	AsLH	0	1	2	0	1	1	1.94
	AsLH ₂	0	1	2	0	1	2	1.59
<i>cys</i>	AsL	1	1	1	1	1	0	4.45
	AsLH	1	1	1	1	1	1	3.31
	AsLH ₂	1	1	1	0	1	1	3.59
<i>tla</i>	AsL	1	1	0	1	1	0	3.33
	AsLH	1	1	0	0	1	0	2.09
<i>tma</i>	AsL	1	2	0	1	2	0	4.41
	AsLH	1	2	0	0	2	0	3.25
	AsLH ₂	1	2	0	0	1	0	2.98
<i>dmsa</i>	AsLH	2	2	0	1	2	0	5.58
	AsLH ₂	2	2	0	0	2	0	5.55
	AsLH ₃	2	2	0	0	1	0	6.10

^{a)} As=As(III), ^{b)} refers to the reaction: As(OH)₃ + HiL (charges omitted for simplicity).

If we consider the amines, a general increase of the stability can also be observed with the increase of the amino groups in the molecule (n_{NH_2}), i.e., from mono- (*etan*) to penta-amine (*tetren*). In this case, it should be taken into account that, over a wide pH range, amino groups are protonated and, likely, an electrostatic interaction occurs between the As(OH)₂O[−] (or H₂AsO₃[−]) and the RNH₃⁺ cation. The electrostatic nature is confirmed by the increase of stability (logK) for the same amine with the increase of the protonation degree ($n_{\text{NH}_3^+}$) and, therefore, of the positive charges on the molecule. Unfortunately, for these systems, the computational calculations, not being able to control the pH and therefore the protonation degree of the amine, did not allow us to reliably simulate the respective interaction modalities.

The increase of stability with the number of carboxylic or amino groups was also observed for amino acids with the increase of logK values from *gly*, which contains one carboxylic and one amino group, to *asp* and to *lys*, which contain a further carboxylic and amino group, respectively.

Finally, to evaluate the effect of the thiol group present only in the *cys* ligand, in Table 2, we also report some recent values referring to the interaction between As(III) and some ligands containing the thiol group, such as *tla*, *tma*, and *dmsa* (Figure 1). As expected, considering the high affinity of As(III) towards -SH groups, the stability of the species was higher with respect to simple -COOH or -NH₂ groups, and logK reached the value of 6.10 (for AsLH₃ species of *dmsa*). As will be shown below, quantum-mechanical calculations executed on a monothiol ligand indicate that, similarly to the carboxylate, S directly bound to As(III) by the displacement of the OH group in As(OH)₃.

The As(III) coordination by the thiol group is stronger than the carboxylic one, even in a competitive situation such as that of cysteine in which thiol, carboxylic, and aminic

groups are simultaneously present. This finding will be quantitatively confirmed by several calculations that we report in the respective subsection (i.e., *Quantum-mechanical calculations*).

To evaluate the relevance of the complex species, comparison between the distributions of As(III) species in two different systems is shown in Figure 2. As for the simultaneous presence of carboxylic and amino groups, two amino acids were chosen: the aspartic acid, which contains a further carboxylic group, and cysteine, in which a thiol group is present. As can be observed, in the As(III)-asp system (Figure 2a), the percentages of species formation were always quite low. Larger were the percentages of the As(III)-cys species (Figure 2b): the presence of the thiol group in the amino acid molecule strongly influenced the distribution and, over all the pH values, As(III) was totally present as a complex species.

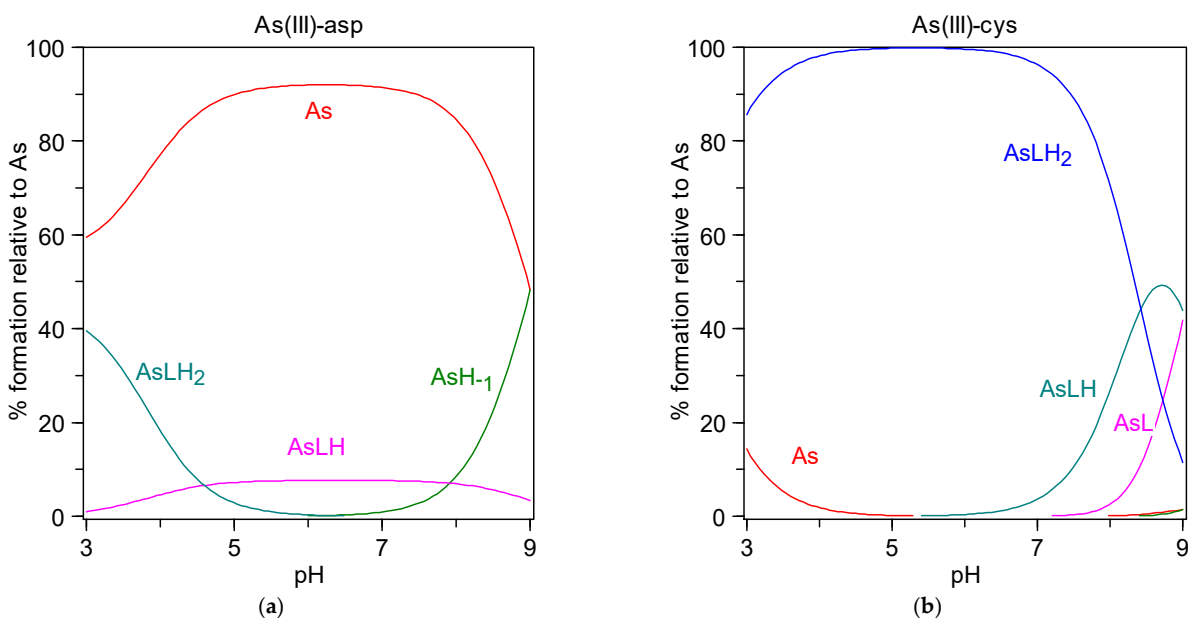


Figure 2. Distribution diagrams of (a) As(III)-asp and (b) As(III)-cys systems. Conditions: $C_{As} = 3$ mmol/L, $C_L = 6$ mmol/L, $I = 0.15$ mol/L (NaCl), $T = 298.15$ K.

3.2. Predictive relationships

Taking into account all values, the formation constants can be modeled by using another approach that considers all the contributions of the functional groups of the ligands under examination (Additivity Factors Approach) [27,28]. Thus, $\log K$ can be written as

$$\log K = \sum n_{x\text{-donor}} \quad (3)$$

where $n_{x\text{-donor}}$ is representative of $-S$, $-N$, or $-O$ donor groups.

For a more accurate analysis of the data, together with the $\log K$ values, in Table 2, we report the number of thiol (n_{SH}), carboxylic (n_{COOH}), and amino (n_{NH_2}) groups of the molecules and, for each species, the number of deprotonated carboxylic (n_{COO^-}), thiol (n_S), and protonated amino ($n_{NH_3^+}$) groups available for the coordination. The latter were obtained considering that the stepwise formation equilibria are referred to the reaction $As(OH)_3 + H_iL$ and, therefore, considering the protonation degree and the form under which the molecules participate to the single reaction.

Considering the data of Table 2 and the comments reported in the previous section, the contribution of each functional group can be represented by the following equation, which takes into account not only the total number of functional groups in the molecule (n_{SH} , n_{COOH} , and n_{NH_2}), but also the number of functional groups available for coordination

(n_{S^-} , n_{COO^-} , and $n_{NH_3^+}$) and, therefore, the charge with which the ligand participates to the stepwise formation reaction:

$$\log K = 2.39(\pm 0.11) n_{SH} + 0.30(\pm 0.07) n_{COOH} + 0.64(\pm 0.08) n_{NH_2} + 0.17(\pm 0.09) (n_{S^-} + n_{COO^-} + n_{NH_3^+}) \quad (4)$$

The equation confirms the experimental results from which it was observed, as expected, that the thiol group mostly contributes to the overall stability of the species. The contribution of the other functional groups is two orders of magnitude lower, but not negligible in the calculation of the stability of the species with polyfunctional ligands. Furthermore, Equation (4) shows that an approximate stability calculation can be performed simply by considering the type and the number of functional groups of the molecule (therefore independently of the pH and of the exact stoichiometry of the species) and, to a lesser extent, the form under which the functional group (protonated or deprotonated, depending on the pH) is present. On the other hand, considering the data in Table 2, we observed that, for the same molecule, no significant differences in stability between the different species were recorded.

Figure 3 shows the stability constant values calculated by means of Equation (4) plotted as a function of the experimental ones. A fairly good agreement is recorded, being the correlation coefficient R^2 equal to 0.92 and the slope equal to 0.97 ± 0.03 . The mean deviation of the calculated $\log K$ value was ± 0.5 , which is relatively high. It is worth emphasizing that Equation (4) allows only for a rough estimate of the stability of the species and that the experimental approach is always highly encouraged for an accurate determination.

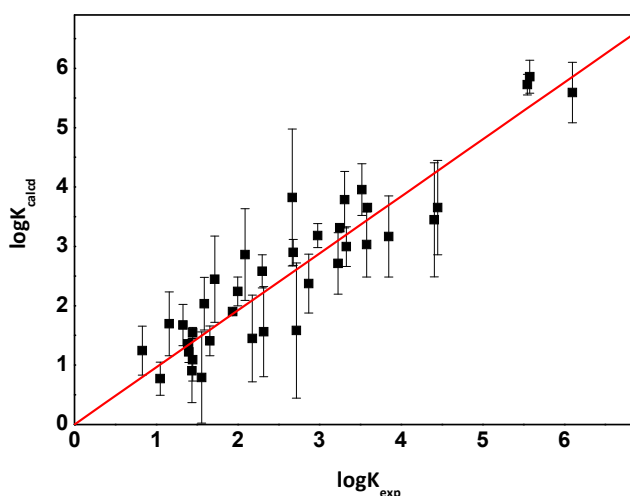


Figure 3. Calculated $\log K$ values for As(III) -S-, -O-, and -N donor ligand interactions vs. experimental ones.

3.3. Quantum-Mechanical Calculations

As anticipated in the Methods section, two main chelation (de-hydration) reactions were considered and characterized. The first one was related to the complexation process of As(III) by involving the thiol functional group (reaction (1)). From quantum-mechanical calculations performed at the B3LYP/6-311++G(d,p) level in the presence of the conductive polarizable continuum model (CPCM) mimicking the water electrostatics, it turns out that a system initially composed of CH_3CH_2SH and arsenous acid ($As(OH)_3$) underwent an energetic advantage (ΔE) of -4.60 kcal/mol upon chelation.

Similarly, but in a limited fashion, reaction (2), involving the complexation of As(III) by means of the carboxylic group, was also exergonic, with $\Delta E = -2.15$ kcal/mol.

However, in such a case, the energetic gain was lower than that recorded for the thiol group case, indicating that this latter group chelated arsenic species more robustly and efficiently than the carboxylic group, a finding adherent with the experimental results. As explained in detail in the Methods section, the respective reaction involving the amino group cannot reliably and quantitatively be characterized by a similar analysis, mainly because of the positively charged nature of NH_3^+ , over a wide pH range. To set the pH in quantum-mechanical simulations, computationally expensive ab initio simulations under explicit solvation similar to those some of ours reported for other systems [26,29–31] will be considered in the future as an extension of the current work.

In order to have a more complete picture shedding some light also to the chelation capabilities of the amino group with respect to the SH and COOH groups, a series of additional calculations at the B3LYP/6-311++G(d,p) level with the CPMC water model was executed. In particular, the cysteine molecule was employed as a prototypical species possessing all the functional groups under investigation. This way, a one-to-one (1,1) interaction with each group at a time with As(III); a two-to-one (2,1) interaction considering each pair of groups simultaneously chelating As(III); and a three-to-one (3,1) interaction, where all the groups actively and simultaneously bind As(III), were considered. Although in this latter case (i.e., the (3,1) interaction), no stable configurations were identified, and the remainder cases allowed for the identification of a fundamental ranking of the binding capabilities of SH, NH_2 , and COOH toward As(III) under ideal conditions.

In fact, optimized molecular structures of the one-to-one (1,1) interaction of As(III) with the three functional groups are shown in Figure 4. The ground-state distance at which arsenic lies when it interacts directly with the thiol group was 2.27 Å (Figure 4a), whereas such a value varied to 2.15 Å and to 1.91 Å in presence of the amino (Figure 4b) and of the carboxylic group (Figure 4c), respectively. Albeit these absolute values give a rough idea of the strength of the formed bonds per se, due to the different natural size of the atoms involved, in each case, these bond lengths have to be rescaled by the Van der Waals radii of the sulfur atom of the thiol group (i.e., 1.83 Å), of the nitrogen atom of the amino group (i.e., 1.62 Å), and of the oxygen atom of the carboxylic group (i.e., 1.37 Å) [32]. The resulting dimensionless coefficient $c=d/r_{vdW}$ provided, indeed, an intuitive and useful measure of the strength of the binding. Of course, at least in principle, the smaller the coefficient, the higher the bond strength. This way, the coefficient associated with the S atom of the thiol group in the (1,1) interaction was equal to 1.24, whilst those of the N atom of the amino and the O atom of the carboxylic groups were equal to 1.34 and 1.39, respectively, as listed in Table 3. In accordance with the experimental findings, such an estimate quantitatively indicates that the thiol group is a better chelating agent than the remainder functional groups under the simplified conditions reproduced in the quantum-mechanical calculations.

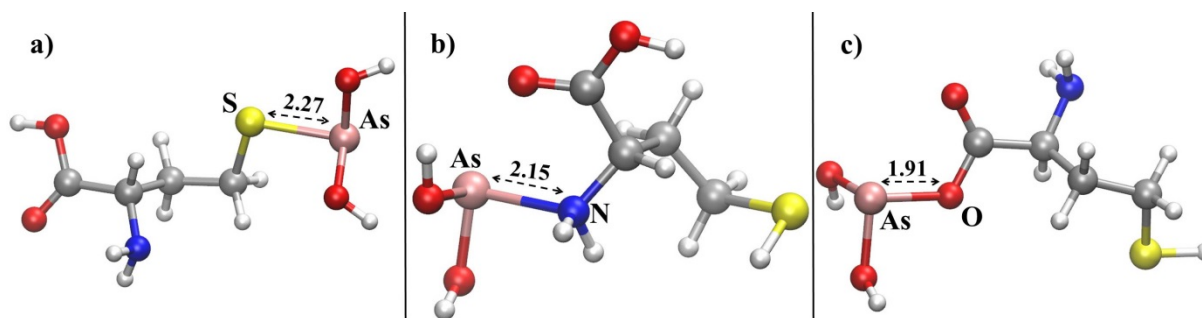


Figure 4. Molecular structures of the complexes formed by the direct one-to-one binding of As(III) with the thiol (a), amino (b), and carboxylic (c) groups optimized at the B3LYP/6-311++G(d,p) under implicit solvation. Relevant optimal interatomic distances are shown in Å.

With the aim of evaluating potential competitive effects exhibited by the investigated groups in cysteine toward the binding of As(III) species, the previous analysis was also conducted considering all permutations of the (2,1) interaction. The quantum-mechanically optimized molecular structures are shown in Figure 5 along with the relevant interatomic distances. The concerted chelation process of As(III) by the thiol and amino groups (Figure 5a) revealed that the arsenic atom lay at a shorter distance from the sulfur atom with respect to the nitrogen atom (i.e., 2.27 Å vs. 2.73 Å). Considering the fact that the size of the S atom is by its own nature larger than that of N, coefficients c equal to 1.24 and 1.69 can be associated to their respective functional groups once the ground-state distances are rescaled by the respective van der Waals radii. In other words, under a competitive situation, the binding capabilities of the thiol group remain unaltered, whilst those of the amino group are further weakened (i.e., c of the N atom was modified from 1.34 to 1.69) by the propensity of the S atom to attract the As(III) one. When the concerted chelation of As(III) by the thiol and the carboxylic groups was taken into account, no significant modifications with respect to the (1,1) interaction were recorded. In fact, once the ground-state distances displayed in Figure 5b were rescaled, coefficients equal to 1.23 and 1.38 were obtained for the SH and the COOH groups, respectively.

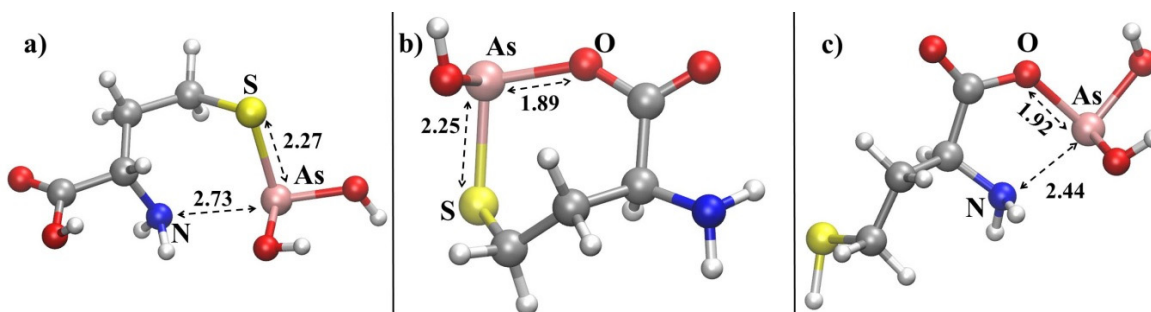


Figure 5. Molecular structures of the complexes formed by the two-to-one binding of As(III) with the thiol and amino (a), thiol and carboxylic (b), and amino and carboxylic (c) groups optimized at the B3LYP/6-311++G(d,p) under implicit solvation. Relevant optimal interatomic distances are shown in Å.

This finding clearly and quantitatively manifests the superior binding capabilities of SH toward As(III) also with respect the COOH group. Incidentally, the fact that the dimensionless coefficients associated with these groups remain substantially unaltered with respect to the (1,1) interactions implicitly indicates the concrete possibility of a simultaneous combined binding of As(III) by the thiol and the carboxylic groups. After all, this kind of chelation modality of arsenic has also been observed in systems such as thiolactic and thiomalic acids when an ab initio treatment of the solvent is employed [14], even though important nuclear quantum effects [33] were overlooked in that analysis.

Finally, Figure 5c shows that under the idealized conditions reproduced in these calculations—completely neglecting the key role played by the pH—the ground-state separation between the nitrogen and the arsenic atoms was larger than that between the oxygen atom of the carboxylic group and As(III). Moreover, once rescaled, these distances reveal that the coefficient c associated with N was equal to 1.51, whereas that of O was 1.40, as summarized in Table 3.

Table 3. Coefficients associated with the binding capabilities of the different functional groups here investigated (SH, COOH, NH₂) in the cysteine molecule and for the (1,1) and (2,1) interaction with As(III).

$c=d/r_{vdw}$	(1,1) Interaction	(2,1) Interaction
SH	1.24	1.23–1.24
COOH	1.39	1.38–1.40
NH ₂	1.34	1.51–1.69

These findings, on the basis of grounded quantum-mechanical calculations that necessarily simplify the complexity of the laboratory experiments, indicated that the thiol group exhibits the best binding capabilities toward As(III) when compared with those offered by the carboxylic and the amino groups. Albeit this was true only for a very simple system such as cysteine and under ideal conditions (no pH variations) and an implicit treatment of the solvent. All these findings are in fairly good agreement with data stemming from laboratory experiments and put these latter on a more quantitative basis.

4. Conclusions

Although the interactions between arsenic (As(III)) and thiol groups are quite established in the literature, potential interactions of As(III) with carboxylic and amino groups, to the best of our knowledge, have never extensively been investigated. With the aim of evaluating the strength underlying the single interactions and, above all, the effects of the simultaneous presence of different functional groups in competitive environmental situations, we here present a study on the interactions established by As(III) with carboxylic acids, amines, and amino acids. Detailed information on these interactions is useful for predictive purpose and, therefore, in all cases (such as removal processes from natural matrices or chelation therapy) in which the knowledge of the form under which arsenic species are present can help to simplify/optimize specific experimental procedures.

Firstly, studies performed on carboxylic and amino ligands have evidenced the formation of simple AsLH_i species with weak formation constants, which slightly increase with increasing the number of carboxylic and/or amino groups in the molecule. The proposed models, determined from experimental measurements performed varying the concentration of arsenic; the concentration of ligands; and, above all, their concentration ratio, provide the possibility to simulate arsenic speciation in any real situation. Moreover, quantum-mechanical calculations, carried out at the B3LYP/6-311++G(d,p) Density Functional Theory (DFT) level and executed on a prototypical monocarboxylic species, have shown that the carboxylate group is able to displace one hydroxyl group in As(OH)₃ and to directly bind to As(III). By contrast, analogous quantum-mechanical calculations on the amino groups have not been useful to characterize the interactions because of the positively charged nature of the amino group (under the protonated NH₃⁺ form) in a wide pH range. This has led us to suppose, on the basis of the obtained experimental results, that an electrostatic interaction occurs between the As(OH)₂O[−] (or H₂AsO₃[−]) and the RNH₃⁺ cation.

Studies on amino acids containing the carboxylic, amino (glycine, aspartic acid, and lysine), and also the thiol group (cysteine) have confirmed that, under a competitive situation where -SH, -COOH, and -NH₂ groups are simultaneously present, the thiol group maintains its superior binding capabilities toward As(III). However, the empirical relationship (4) useful for a rough estimate of the stability of the species evidenced that, despite the thiol group mostly contributing to the stability of the species, the contribution of the other functional groups is two orders of magnitude lower, but not negligible for the calculation of the total stability of the species with polyfunctional ligands. Quantum-mechanical calculations performed on cysteine as a prototypical species containing the thiol, carboxylic, and amino groups indicate the concrete possibility of a simultaneous combined binding of As(III) by the thiol and the carboxylic groups. Finally, the superior capabilities of the sulfur atom of the thiol group in directly binding As(III) with respect to the atoms of the carboxylic and amino groups were quantitatively witnessed, within this DFT-based analysis, both under a simple direct interaction and under competitive more complex chelation modalities. On the other hand, the possibility of the simultaneous chelation of As(III) by the three functional groups here investigated was ruled out by the current calculations.

Supplementary Materials: The following supporting information can be downloaded at <https://www.mdpi.com/article/10.3390/app12063210/s1>, Table S1: As(III) hydrolysis and ligand protonation constants at $I = 0.15$ mol/L (NaCl) and $T = 298.15$ K.

Author Contributions: Conceptualization, C.F. and G.C.; methodology, C.F., G.C., O.G., D.C., and V.M.-N.; software, G.C. and V.M.-N.; investigation, D.C., O.G., R.C.P., F.S., and S.T.; resources, J.S.; data curation, C.F., G.C., O.G., D.C., and V.M.-N.; writing—original draft preparation, C.F., D.C., and G.C.; writing—review and editing C.F., G.C., and O.G.; supervision, C.F. and G.C. All authors have read and agreed to the published version of the manuscript.

Funding: This research received no external funding.

Institutional Review Board Statement: Not applicable.

Informed Consent Statement: Not applicable.

Data Availability Statement: The data presented in this study are available on request from the corresponding authors.

Conflicts of Interest: The authors declare no conflicts of interest.

References

1. Björklund, G.; Oliinyk, P.; Lysiuk, R.; Rahaman, M.S.; Antonyak, H.; Lozynska, I.; Lenchyk, L.; Peana, M. Arsenic intoxication: General aspects and chelating agents. *Arch. Toxicol.* **2020**, *94*, 1879–1897.
2. Hettick, B.E.; Cañas-Carrell, J.E.; French, A.D.; Klein, D.M. Arsenic: A Review of the Element's Toxicity, Plant Interactions, and Potential Methods of Remediation. *J. Agric. Food Chem.* **2015**, *63*, 7097–7107.
3. Masuda, H. Arsenic cycling in the Earth's crust and hydrosphere: Interaction between naturally occurring arsenic and human activities. *Prog. Earth Planet. Sci.* **2018**, *5*, 68.
4. Sharma, V.K.; Sohn, M. Aquatic arsenic: Toxicity, speciation, transformations, and remediation. *Environ. Int.* **2009**, *35*, 743–759.
5. Morales-Simfors, N.; Bundschuh, J. Arsenic-rich geothermal fluids as environmentally hazardous materials—A global assessment. *Sci. Total Environ.* **2022**, *817*, 152669.
6. International Agency for Research on Cancer (IARC). *Arsenic, Metals, Fibres and Dusts*; International Agency for Research on Cancer (IARC): Lyon, France, 2012.
7. Chakraborty, A.; Ghosh, S.; Biswas, B.; Pramanik, S.; Nriagu, J.; Bhowmick, S. Epigenetic modifications from arsenic exposure: A comprehensive review. *Sci. Total Environ.* **2022**, *810*, 151218.
8. Merian, E.; Anke, M.; Ihnat, M.; Stoeppeler, M. *Elements and Their Compounds in the Environment: Occurrence, Analysis and Biological Relevance*; WILEY-VCH Verlag GMBH and Co., KGaA: Weinheim, Germany, 2004.
9. Bashir, A.; Pandith, A.H.; Malik, L.A.; Qureshi, A.; Ganaie, F.A.; Dar, G.N. Magnetically recyclable L-cysteine capped Fe₃O₄ nanoadsorbent: A promising pH guided removal of Pb(II), Zn(II) and HCrO₄—Contaminants. *J. Environ. Chem. Eng.* **2021**, *9*, 105880.
10. Chillè, D.; Aiello, D.; Grasso, G.I.; Giuffrè, O.; Napoli, A.; Sgarlata, C.; Foti, C. Complexation of As(III) by phosphonate ligands in aqueous fluids: Thermodynamic behavior, chemical binding forms and sequestering abilities. *J. Environ. Sci.* **2020**, *94*, 100–110.
11. Foti, C.; Mineo, P.G.; Nicosia, A.; Scala, A.; Neri, G.; Piperno, A. Recent Advances of Graphene-Based Strategies for Arsenic Remediation. *Front. Chem.* **2020**, *14*, 608236.
12. Templeton, D.M.; Ariese, F.; Cornelis, R.; Danielsson, L.G.; Muntau, H.; Van Leeuwen, H.P.; Lobinski, R. Guidelines for terms related to chemical speciation and fractionation of elements. Definitions, structural aspects, and methodological approaches (IUPAC Recommendations 2000). *Pure Appl. Chem.* **2000**, *72*, 1453–1470.
13. Sowers, T.D.; Nelson, C.M.; Blackmon, M.D.; Jerden, M.L.; Kirby, A.M.; Diamond, G.L.; Bradham, K.D. Interconnected soil iron and arsenic speciation effects on arsenic bioaccessibility and bioavailability: A scoping review. *J. Toxicol. Environ. Health Pt. B* **2022**, *25*, 1–22.
14. Cassone, G.; Chillè, D.; Giacobello, F.; Giuffrè, O.; Mollica Nardo, V.; Ponterio, R.C.; Saija, F.; Sponer, J.; Trusso, S.; Foti, C. Interaction between As(III) and Simple Thioacids in Water: An Experimental and ab Initio Molecular Dynamics Investigation. *J. Phys. Chem. B* **2019**, *123*, 6090–6098.
15. Chillè, D.; Cassone, G.; Giacobello, F.; Giuffrè, O.; Mollica Nardo, V.R.C.P.; Saija, F.; Sponer, J.; Trusso, S.; Foti, C. Removal of As(III) from Biological Fluids: Mono- versus Dithiolic Ligands. *Chem. Res. Toxicol.* **2020**, *33*, 967–974.
16. Solmi, M.V.; Schmitz, M.; Leitner, W. CO₂ as a Building Block for the Catalytic Synthesis of Carboxylic Acids. *Stud. Surf. Sci. Catal.* **2019**, *178*, 105–124.
17. Yu, R.J.; Van Scott, E.J. Alpha-hydroxyacids and carboxylic acids. *J. Cosmet. Dermatol.* **2004**, *3*, 76–87.
18. Li, P.; He, W.; Wu, G. Composition of amino acids in foodstuffs for humans and animals. In *Amino Acids in Nutrition and Health—Advances in Experimental Medicine and Biology*; Wu, G., Ed.; Springer: Berlin/Heidelberg, Germany, 2021; Volume 1332.
19. De Stefano, C.; Sammartano, S.; Mineo, P.; Rigano, C. Computer tools for the speciation of natural fluids. In *Marine Chemistry—An Environmental Analytical Chemistry Approach*; Gianguzza, A.; Pelizzetti, E.; Sammartano, S., Eds.; Kluwer Academic Publishers: Amsterdam, The Netherlands, 1997; pp. 71–83.

20. Frisch, M.J. *Gaussian 09, Revision A.02*; Gaussian, Inc.: Wallingford, CT, USA, 2009.
21. Becke, A.D. Density-functional exchange-energy approximation with correct asymptotic behavior. *Phys. Rev. A* **1988**, *38*, 3098.
22. Lee, V.; Yang, W.; Parr, R.G. Development of the Colle-Salvetti correlation-energy formula into a functional of the electron density. *Phys. Rev. B* **1988**, *37*, 785.
23. Stephens, P.J.; Devlin, F.J.; Chabalowski, C.F.; Frisch, M.J. Ab Initio Calculation of Vibrational Absorption and Circular Dichroism Spectra Using Density Functional Force Fields. *J. Phys. Chem.* **1994**, *98*, 11623–11627.
24. Vosko, S.H.; Wilk, L.; Nusair, M. Accurate Spin-Dependent Electron Liquid Correlation Energies for Local Spin Density Calculations: A Critical Analysis. *Can. J. Phys.* **1980**, *58*, 1200–1211.
25. Tomasi, J.; Mennucci, B.; Cammi, R. Quantum Mechanical Continuum Solvation Model. *Chem. Rev.* **2005**, *105*, 2999–3094.
26. Cassone, G.; Chillè, D.; Foti, C.; Giuffrè, O.; Ponterio, R.C.; Sponer, J.; Saija, F. Stability of hydrolytic arsenic species in aqueous solutions: As^{3+} vs. As^{5+} . *Phys. Chem. Chem. Phys.* **2018**, *20*, 23272–23280.
27. Cardiano, P.; Giacobello, F.; Giuffrè, O.; Sammartano, S. Thermodynamics of Al^{3+} -thiocarboxylate interaction in aqueous solution. *J. Mol. Liq.* **2016**, *222*, 614–621.
28. Cucinotta, D.; De Stefano, C.; Giuffrè, O.; Lando, G.; Milea, D.; Sammartano, S. Formation, stability and empirical relationships for the binding of Sn^{2+} by O-, N- and S- donor ligands. *J. Mol. Liquids* **2014**, *200*, 329–339.
29. Cassone, G.; Creazzo, F.; Giaquinta, P.V.; Saija, F.; Saitta, A.M. Ab initio molecular dynamics study of an aqueous NaCl solution under an electric field. *Phys. Chem. Chem. Phys.* **2016**, *18*, 23164–23173.
30. Cassone, G.; Sofia, A.; Rinaldi, G.; Sponer, J. Catalyst-free hydrogen synthesis from liquid ethanol: An ab initio molecular dynamics study. *J. Phys. Chem. C* **2019**, *123*, 9202–9208.
31. Cassone, G.; Sofia, A.; Sponer, J.; Saitta, A.M.; Saija, F. Ab initio molecular dynamics study of methanol-water mixtures under external electric fields. *Molecules* **2020**, *25*, 3371.
32. Mantina, M.; Chamberlin, A.C.; Valero, R.; Cramer, C.J.; Truhlar, D.G. Consistent van der Waals radii for the whole main group. *J. Phys. Chem. A* **2009**, *113*, 5806–5812.
33. Cassone, G. Nuclear Quantum Effects largely influence molecular dissociation and proton transfer in liquid water under an electric field. *J. Phys. Chem. Lett.* **2020**, *11*, 8983–8988.